ATLAS NOTE

ATLAS-CONF-2012-002

February 11, 2012

Search for Events with Large Missing Transverse Momentum, Jets, and at Least Two Tau Leptons in 7 TeV Proton-Proton Collision Data with the ATLAS Detector

The ATLAS Collaboration

ATLAS-CONF-2012-002
14/02/2012

Abstract

A search for events with large missing transverse momentum, jets, and at least two taus has been performed using $2\,\text{fb}^{-1}$ of proton-proton collision data at $\sqrt{s} = 7\,\text{TeV}$ recorded with the ATLAS detector at the Large Hadron Collider. No excess above the Standard Model background expectation is observed and a 95 % CL visible cross section upper limit for new phenomena of 2.9 fb is set. For a minimal model of gauge-mediated supersymmetry breaking (GMSB), limits on the production cross section are set. A 95 % CL lower limit of 32 TeV is set on the GMSB breaking scale Λ independent of $\tan\beta$. These limits provide the most stringent tests in a large part of the considered parameter space to date.

1 Introduction

Supersymmetry (SUSY) [1–5] introduces a symmetry between fermions and bosons, resulting in a SUSY partner (sparticle) with identical quantum numbers except a difference by half a unit of spin for each Standard Model (SM) particle. As none of these sparticles have been observed, SUSY must be a broken symmetry if realised in nature. Assuming R-parity conservation [6, 7], sparticles are produced in pairs. These would then decay through cascades involving other sparticles until the lightest SUSY particle (LSP) is produced, which is stable.

Minimal gauge-mediated supersymmetry breaking (GMSB) [8–12] models can be described by six parameters: the SUSY breaking mass scale felt by the low-energy sector (Λ), the messenger mass ($M_{\rm mess}$), the number of SU(5) messengers (N_5), the ratio of the vacuum expectation values of the two Higgs doublets ($\tan\beta$), the Higgs sector mixing parameter (μ), and the scale factor for the gravitino mass ($C_{\rm grav}$). In this analysis Λ and $\tan\beta$ are treated as free parameters and the other parameters are fixed to $M_{\rm mess} = 250\,\text{TeV}$, $N_5 = 3$, $\mu > 0$, and $C_{\rm grav} = 1$. The latter determines the lifetime of the next-to-lightest SUSY particle (NLSP). For $C_{\rm grav} = 1$ the NLSP decays promptly ($c\tau_{\rm NLSP} < 0.1\,\text{mm}$). With these parameters, the production of squark and/or gluino pairs is expected to dominate at the present Large Hadron Collider (LHC) energy. These sparticles then decay directly or through cascades into the NLSP, which subsequently decays to the LSP. In GMSB models, the LSP is the gravitino ($\tilde{G}$), which couples exclusively to the NLSP due to its very small mass of O(keV). This leads to multiple jets and missing transverse momentum ($E_{\rm T}^{\rm miss}$) in the final states. The experimental signature is then largely determined by the nature of the NLSP, which can be either the lightest stau ($\tilde{\tau}$), the right handed slepton ($\tilde{\ell}$), the lightest neutralino ($\tilde{\chi}_1^0$), or the sneutrino ($\tilde{\nu}$), leading to final states containing taus, leptons ($\ell = e, \mu$), photons, b-jets, or neutrinos. For $N_5 = 3$ the $\tilde{\tau}$ and $\tilde{\ell}$ regions are enhanced compared to lower values of N_5. At large values of $\tan\beta$, the $\tilde{\tau}$ is the NLSP for most of the parameter space, which leads to final states containing between two and four tau leptons.

This note reports on the search for events with large $E_{\rm T}^{\rm miss}$, jets, and at least two hadronically decaying tau leptons. It has been performed using $2\,\text{fb}^{-1}$ of proton-proton (pp) collision data at $\sqrt{s} = 7\,\text{TeV}$ recorded with the ATLAS detector at the LHC between March and August 2011. The results are interpreted in the context of a minimal GMSB model. All four LEP Collaborations studied $\tilde{\tau}$ pair production, with the subsequent decay $\tilde{\tau} \to \tau\tilde{G}$ in the minimal GMSB model. For prompt decays, $\tilde{\tau}$ NLSPs with masses below 87 GeV are excluded [13]. The OPAL experiment set a limit on the SUSY breaking mass scale Λ of 26 TeV for $N_5 = 3$ and $M_{\rm mess} = 250\,\text{TeV}$ independent of $\tan\beta$ and the NLSP lifetime [14]. The CMS Collaboration searched for new physics in same-sign ditau events [15] and multi-lepton events including ditaus [16] using $35\,\text{pb}^{-1}$ of data. Preliminary results have also been published in [17], [18] and [19], using $2.1\,\text{fb}^{-1}$, $1\,\text{fb}^{-1}$ and $0.98\,\text{fb}^{-1}$ of data, respectively. The minimal GMSB model was not considered in the limit setting.

2 ATLAS detector

The ATLAS detector [20] is a multi-purpose apparatus with a forward-backward symmetric cylindrical geometry and nearly 4π solid angle coverage. The inner tracking detector (ID) consists of a silicon pixel detector, a silicon strip detector, and a transition radiation tracker. The ID is surrounded by a thin superconducting solenoid providing a 2 T magnetic field and by fine-granularity lead/liquid-argon (LAr) electromagnetic calorimeters. An iron/scintillating-tile calorimeter provides hadronic coverage in the central rapidity[1] range. The endcap and forward regions are instrumented with liquid-argon calorimeters

[1] ATLAS uses a right-handed coordinate system with its origin at the nominal interaction point (IP) in the centre of the detector and the z-axis along the beam pipe. The x-axis points from the IP to the centre of the LHC ring, and the y-axis points upward. Cylindrical coordinates (R, ϕ) are used in the transverse plane, ϕ being the azimuthal angle around the beam pipe. The

for both electromagnetic and hadronic measurements. An extensive muon spectrometer system that incorporates large superconducting toroidal magnets surrounds the calorimeters.

3 Simulated samples

Monte Carlo (MC) simulations are used to extrapolate backgrounds from control regions (CR) to the signal region (SR) and to evaluate the efficiencies for the SUSY models considered. Samples of W and Z/γ^* production with accompanying jets are simulated with ALPGEN [21], using CTEQ6L1 [22] parton density functions (PDFs). Top quark pair production, single top production and diboson pair production are simulated with MC@NLO [23–25] and the next-to-leading order (NLO) PDF set CTEQ6.6 [26]. The production of QCD multijet events is simulated with PYTHIA [27]. Fragmentation and hadronisation are performed with HERWIG [28], using JIMMY [29] for the underlying event simulation and the ATLAS MC10 parameter tune [30]. The programs TAUOLA [31, 32] and PHOTOS [33] are used to model the decays of τ leptons and the radiation of photons, respectively.

For the minimal GMSB model considered in this analysis, the SUSY mass spectra are calculated using ISAJET 7.80 [34]. The MC signal samples are produced using HERWIG++ 2.4.2 [35] with MRST2007 LO* [36] PDFs. NLO cross sections are calculated using PROSPINO 2.1 [37–42].

All samples are processed through the GEANT4-based simulation [43] of the ATLAS detector [44]. The variation of the number of pp interactions per bunch crossing (pile-up) as a function of the instantaneous luminosity is taken into account by weighting the simulated number of overlaid minimum bias events according to the observed distribution of the number of pile-up interactions in data, ranging between four and eight.

4 Object reconstruction

Jets are reconstructed using the anti-k_t jet clustering algorithm [45] with radius parameter $R = 0.4$. Their energies are calibrated to correct for calorimeter non-compensation, upstream material, and other effects [46]. Jets are required to have transverse momentum (p_{T}) above 20 GeV and $|\eta| < 2.5$.

The reconstruction and identification of electron (using the "medium" working point) and muon candidates is described in Refs. [47] and [48], respectively.

The measurement of the missing transverse momentum two-dimensional vector $p_{\mathrm{T}}^{\mathrm{miss}}$ (and its magnitude $E_{\mathrm{T}}^{\mathrm{miss}}$) is based on the transverse momenta of identified jets, electrons, muons, and all calorimeter clusters with $|\eta| < 4.5$ not associated to such objects [49].

In this search, only hadronically decaying taus are considered. The tau reconstruction is seeded from anti-k_t jets with $p_{\mathrm{T}} > 10$ GeV. An η and p_{T}-dependent energy calibration to the hadronic tau energy scale is applied. Hadronic tau identification is based on observables sensitive to the transverse and longitudinal shape of the calorimeter shower and on tracking information, combined in a boosted decision tree (BDT) discriminator [50]. Transition radiation and calorimeter information is used for vetoing electrons misreconstructed as taus. A tau candidate must have $p_{\mathrm{T}} > 20$ GeV, $|\eta| < 2.5$, and one or three associated tracks of $p_{\mathrm{T}} > 1$ GeV with a charge sum of ± 1. The efficiency of the BDT tau identification ("loose" working point in Ref. [50]), computed on $Z \to \tau\tau$ events, is about 60 %, independent of p_{T}, while achieving a jet background rejection factor of 20 – 50.

During a part of the data-taking period, an electronics failure in the LAr barrel EM calorimeter created a dead region in the second and third layers, corresponding to approximately 1.4×0.2 rad in $\Delta\eta \times \Delta\phi$. Electron and tau candidates falling in this region are discarded. A correction to the jet energy is made using the energy depositions in the cells neighbouring the dead region; events having at least one

pseudorapidity is defined in terms of the polar angle θ as $\eta = -\ln\tan(\theta/2)$.

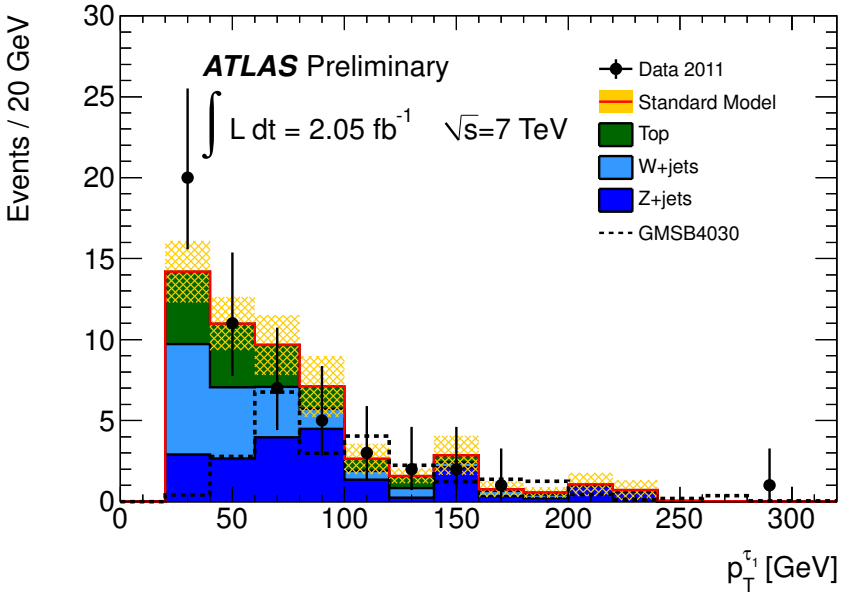

Figure 1: The p_{T} spectrum of the leading tau candidates in data (points, statistical uncertainty only) and the estimated SM background after the pre-selection of candidate events, soft multi-jet rejection, and the requirement of two or more taus. The yellow band centered around the total SM background indicates the statistical uncertainty. Also shown is the expected signal from a typical GMSB ($\Lambda = 40\,\mathrm{TeV}, \tan\beta = 30$) sample.

jet for which the energy after correction is above 30 GeV are discarded, resulting in a loss of $\sim 7\%$ of the data sample.

5 Data analysis

The analysed data sample, after applying beam, detector and data-quality requirements, corresponds to an integrated luminosity of $(2.05 \pm 0.08)\,\mathrm{fb}^{-1}$ [51, 52]. Candidate events are pre-selected by a trigger requiring a leading jet with $p_{\mathrm{T}} > 75\,\mathrm{GeV}$, measured at the raw electromagnetic scale, and missing transverse momentum above 45 GeV. In the offline analysis, these events are then required to have a reconstructed primary vertex with at least five tracks, a leading jet with p_{T} above 130 GeV and $E_{\mathrm{T}}^{\mathrm{miss}} > 130\,\mathrm{GeV}$. These requirements ensure a uniform trigger efficiency that exceeds 98 %.

Pre-selected events are required to have at least two identified tau candidates, and must not contain any electron or muon candidate with transverse momenta above 20 GeV and 10 GeV, respectively. To suppress soft multi-jet events, a second jet with $p_{\mathrm{T}} > 30\,\mathrm{GeV}$ is required. The p_{T} spectrum of the leading tau candidate after candidates selection, soft multi-jet rejection, and the requirement of two or more taus is shown in Fig. 1.

This selection rejects almost all multi-jet background events. Remaining multi-jet events, where highly energetic jets are mis-measured, are rejected by requiring the azimuthal angle between the missing transverse momentum and either of the two leading jets $\Delta\phi(E_{\mathrm{T}}^{\mathrm{miss}}, \mathrm{jet}_{1,2})$ to be larger than 0.4 rad.

The SR is defined by requiring $m_{\mathrm{eff}} > 700\,\mathrm{GeV}$ and $m_T^{\tau 1} + m_T^{\tau 2} > 80\,\mathrm{GeV}$, where m_{eff} is the effective

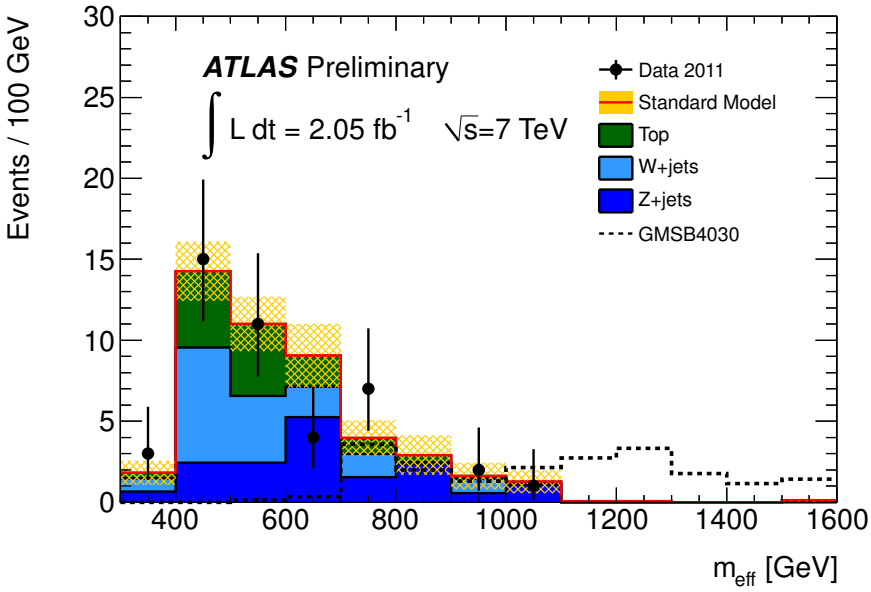

(a) m_{eff} distribution after the $\Delta\phi$ requirement

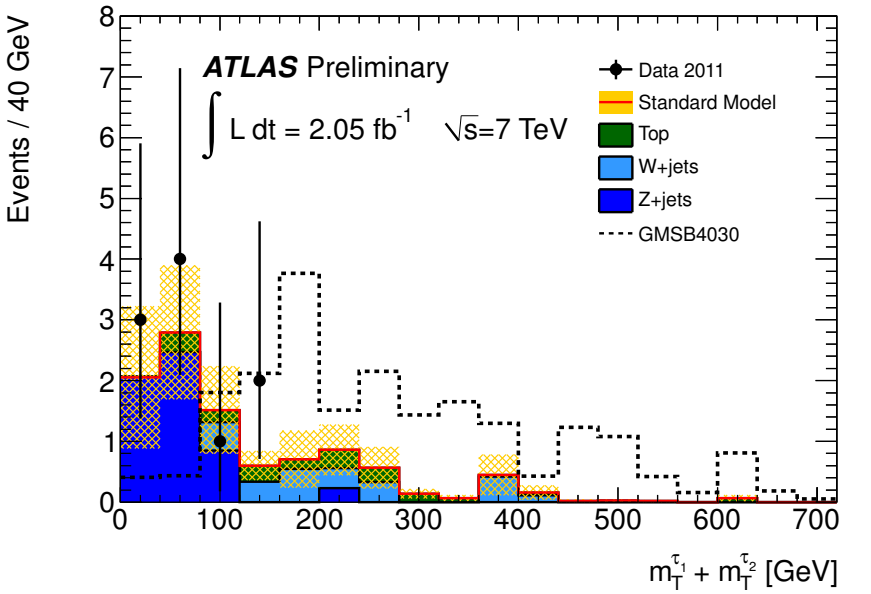

(b) $m_T^{\tau 1} + m_T^{\tau 2}$ distribution after the m_{eff} requirement

Figure 2: Distributions of variables used for the signal region definition in data (points, statistical uncertainty only) and the estimated SM background after the pre-selection of candidate events, soft multi-jet rejection and the requirement of two or more taus. The yellow band centered around the total SM background indicates the statistical uncertainty. Also shown is the expected signal from a typical GMSB ($\Lambda = 40\,\text{TeV}, \tan\beta = 30$) sample.

mass[2] and $m_T^{\tau 1} + m_T^{\tau 2}$ is the sum of the transverse masses[3] of the two leading tau candidates.

The m_{eff} distribution after the $\Delta\phi(E_{\text{T}}^{\text{miss}}, \text{jet}_{1,2})$ requirement and the $m_T^{\tau 1} + m_T^{\tau 2}$ distribution after the m_{eff} requirement are shown in Fig. 2. After applying all the analysis requirements, 3 events are selected in the data.

6 Background estimation

The dominant backgrounds in the SR are from top-pair + single top events ($t\bar{t}$) and $W \to \tau\nu_\tau$ events, in which one real tau is correctly reconstructed and the other tau candidates are mis-reconstructed from hadronic activity in the final state. This background contribution is determined in a CR defined by inverting the m_{eff} cut. Owing to the $\Delta\phi$ requirement and the request of two or more taus, the CR has negligible contamination from QCD multi-jet events. The MC overestimates the number of events in the CR compared to data, due to mis-modeling of tau mis-reconstruction probabilities. MC studies show that the tau mis-reconstruction probability is, to good approximation, independent of m_{eff}, so that the measured ratio of the data to MC event yields in the CR can be used to correct the MC background prediction in the SR.

In a similar way, the QCD multi-jet background expectation is computed in a QCD multi-jet dominated CR defined by inverting the $\Delta\phi$ and m_{eff} cuts. In addition, $E_{\text{T}}^{\text{miss}}/m_{\text{eff}} < 0.4$ is required to increase the purity of this CR sample. The extrapolated contribution of this background source to the SR is found to be negligible.

$Z \to \tau\tau$ events, with both taus correctly reconstructed, also contribute to the total background in this analysis. This background is determined using MC simulated events.

7 Background systematic uncertainties

The theoretical uncertainty on the MC-based corrected extrapolation of the W and $t\bar{t}$ backgrounds from the CR into the SR is estimated using alternative MC samples obtained by varying simultaneously the renormalisation and factorisation scales between half and twice their default values. An uncertainty of 14 % is estimated from this procedure. Moreover, an uncertainty of 23 % is associated to the normalisation factor derived in the CR. This uncertainty is estimated by repeating the normalisation to data independently for W and $t\bar{t}$.

Systematic uncertainties on the jet energy scale and jet energy resolution [46] are applied on MC to the selected jets and propagated throughout the analysis, including to $E_{\text{T}}^{\text{miss}}$. The difference in the number of expected background events obtained with the nominal MC simulation and after applying these changes is taken as systematic uncertainty, and corresponds to 18 % each. The effect of the systematic uncertainty on the tau energy on the expected background is estimated in a similar way and results in a value of 7 %. The uncertainties from the jet and tau energy scale are treated as fully correlated. The uncertainties on the estimate of the backgrounds due to the uncertainties on the tau identification efficiency and mis-reconstruction rate depend on the tau identification algorithm used in the analysis, the kinematics of the τ sample, and the number of associated tracks. They are found to be 2.5 % and 0.5 %, respectively. The systematic uncertainty associated to pile-up simulation in MC is 1 %. The uncertainty due to the luminosity uncertainty [51, 52] is 0.8 %. The contributions from the different systematic uncertainties result in a total background systematic uncertainty of 41 %.

[2]The effective mass m_{eff} is calculated as the sum of $E_{\text{T}}^{\text{miss}}$ and the magnitude of the transverse momenta of the two highest-p_{T} jets and all selected taus.

[3]The transverse mass m_{T} formed by $E_{\text{T}}^{\text{miss}}$ and the p_{T} of the tau lepton (τ) is defined as $m_{\text{T}} = \sqrt{2p_{\text{T}}^{\tau}E_{\text{T}}^{\text{miss}}(1 - \cos(\Delta\phi(\tau, p_{\text{T}}^{\text{miss}})))}$.

In total 5.3 ± 1.3(stat) ± 2.2(sys) background events are expected where the first uncertainty is statistical and includes the statistical component of the background correction factor uncertainty, and the second is systematic. Roughly half of the background is composed of $t\bar{t}$ events, and the other half is evenly split into W and Z events with accompanying jets.

8 Signal efficiencies and systematic uncertainties

GMSB signal samples were generated on a grid ranging from $\Lambda = 10\,\text{TeV}$ to $\Lambda = 80\,\text{TeV}$ and from $\tan\beta = 2$ to $\tan\beta = 50$. The number of selected events decreases significantly with increasing Λ due to the steep decrease of the cross section. The cross section drops continuously from 22 pb for $\Lambda = 15\,\text{TeV}$ to 5.0 fb for $\Lambda = 80\,\text{TeV}$. The selection efficiency is highest ($\approx 3\%$) for high $\tan\beta$ and lower Λ values including the region of the GMSB4030 point (GMSB4030, $\Lambda = 40$, $\tan\beta = 30$) which is near the expected limit. It drops to 0.2 % in the non-stau NLSP regions and for high Λ values. This is primarily a consequence of the light lepton veto and the requirement of two hadronically decaying taus, respectively.

The total systematic uncertainty on the signal selection from the systematic uncertainties discussed in Section 7 ranges between 7.5 % and 36 % over the GMSB grid. The statistical uncertainty from the limited size of the MC signal samples lies between 7.6 % and 59 %. This yields $20.8 \pm 3.4(\text{stat}) \pm 5.4(\text{sys})$ signal events for a typical GMSB model point. Theory uncertainties related to the GMSB cross section predictions are estimated through variations of the factorisation and renormalisation scales in the NLO `PROSPINO` calculation between half and twice their default values, by considering variations in α_s, and by considering the PDF uncertainties using the `CTEQ6.6M` PDF error sets [53]. These uncertainties are calculated for individual SUSY production processes and for each point in the signal grid, leading to overall theoretical cross section uncertainties between 6.5 % and 22 %.

9 Results

Based on the observation of 3 events in the SR, and a background expectation of $5.3 \pm 1.3(\text{stat}) \pm 2.2(\text{sys})$ events, a 5.9 (7.0) events observed (expected) upper limit at 95 % Confidence Level (CL) is set on the number of events from any scenario of physics beyond the SM in the SR using the profile likelihood and CL_s method [54]. Uncertainties on the background and signal expectations are treated as Gaussian-distributed nuisance parameters in the likelihood fit. This limit translates into a 95 % observed (expected) upper limit of 2.9 fb (3.4 fb) on the visible cross section for new phenomena, defined by the product of cross section, branching fraction, acceptance, and efficiency. Upper limits at 95 % CL ranging between 95 fb and 9.0 pb are obtained for the production cross sections of the GMSB models considered here, as shown in Fig. 3. These limits include all systematic uncertainties except for the theoretical uncertainties affecting the signal cross sections.

The expected and observed 95 % CL limits on the GMSB model parameters Λ and $\tan\beta$ are shown in Fig. 4 including the lower limits from LEP [13] and OPAL [14] for comparison. These limits are calculated including all experimental and theoretical uncertainties on the background and signal expectations. Excluding the theoretical uncertainties on the signal cross section from the limit calculation has a negligible effect on the limits obtained. The best exclusion is set for $\Lambda = 47\,\text{TeV}$ and $\tan\beta = 37$. All values of $\Lambda < 32\,\text{TeV}$ are excluded at 95 % CL, independently of $\tan\beta$.

10 Conclusions

A search for events with two or more hadronically decaying tau leptons, large $E_{\text{T}}^{\text{miss}}$, and jets is performed using $2\,\text{fb}^{-1}$ of $\sqrt{s} = 7\,\text{TeV}$ pp collision data recorded with the ATLAS detector at the LHC. Three

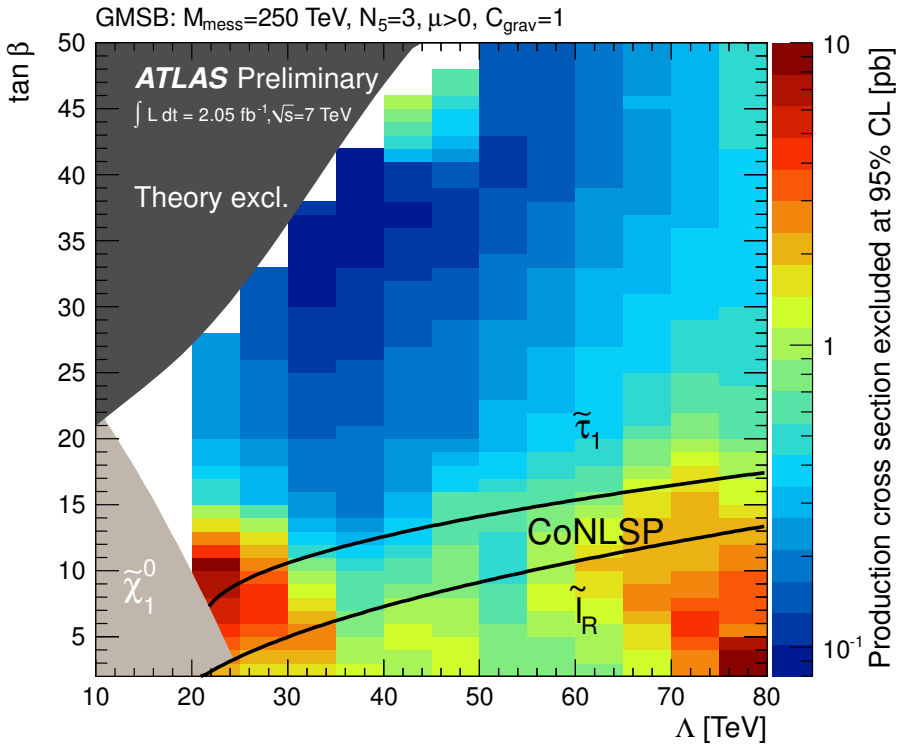

Figure 3: Observed 95 % CL upper limits on the production cross section for the minimal GMSB model parameters Λ and $\tan\beta$ for $\tilde{\tau}$ and $\tilde{\ell}$ NLSP. The dark grey area indicates the region which is theoretically excluded due to unphysical sparticle masses. The light grey area indicates the region where the NLSP is the neutralino, which is not considered here. In the CoNLSP region, the mass difference between the $\tilde{\tau}$ and $\tilde{\ell}$ is smaller than the tau lepton mass, allowing them both to be the NLSP. Further model parameters are $M_{\text{mess}} = 250\,\text{TeV}$, $N_5 = 3$, $\mu > 0$, and $C_{\text{grav}} = 1$.

events are found, consistent with the expected SM background. The results are used to set a model-independent 95 % CL upper limit of 5.9 events from new phenomena, corresponding to an upper limit on the visible cross section of 2.9 fb. Limits on the production cross sections and model parameters are set for a minimal GMSB model. The limit on the SUSY breaking scale, Λ, of 32 TeV is determined, independently of $\tan\beta$. It increases up to 47 TeV for $\tan\beta = 37$. These results provide the most stringent tests in a large part of the parameter space considered to date, improving previous best limits from LEP [13] and OPAL [14].

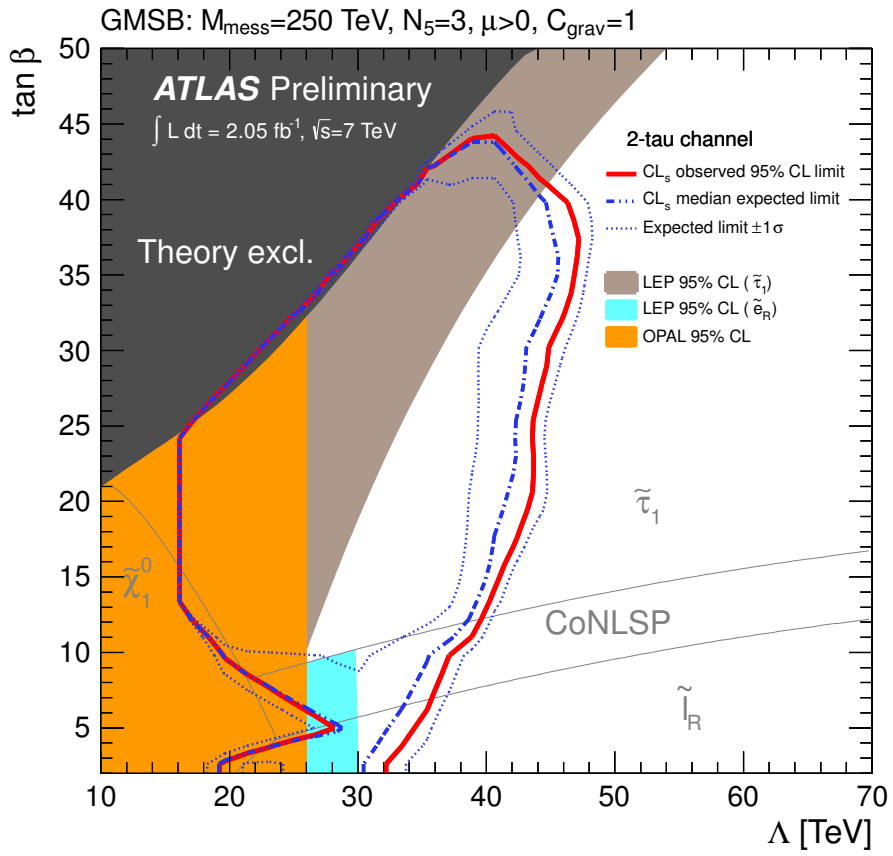

Figure 4: Expected and observed 95 % CL limits on the minimal GMSB model parameters Λ and $\tan\beta$ for $\tilde{\tau}$ and $\tilde{\ell}$ NLSP. The dark grey area indicates the region which is theoretically excluded due to unphysical sparticle masses. In the CoNLSP region, the mass difference between the $\tilde{\tau}$ and $\tilde{\ell}$ is smaller than the tau lepton mass, allowing them both to be the NLSP. Further model parameters are $M_{\text{mess}} = 250\,\text{TeV}$, $N_5 = 3$, $\mu > 0$, and $C_{\text{grav}} = 1$. The previous LEP [13] and OPAL [14] limits are also shown.

References

[1] Y. A. Golfand and E. P. Likhtman, *Extension of the Algebra of Poincare Group Generators and Violation of p Invariance*, JETP Lett. **13** (1971) 323.

[2] A. Neveu and J. H. Schwarz, *Factorizable Dual Model of Pions*, Nucl. Phys. **B31** (1971) 86.

[3] P. Ramond, *Dual Theory for Free Fermions*, Phys. Rev. **D3** (1971) 2415.

[4] D. V. Volkov and V. P. Akulov, *Is the Neutrino a Goldstone Particle?*, Phys. Lett. **B46** (1973) 109.

[5] J. Wess and B. Zumino, *Supergauge Transformations in Four-Dimensions*, Nucl. Phys. **B70** (1974) 39.

[6] P. Fayet, *Spontaneously Broken Supersymmetric Theories of Weak, Electromagnetic and Strong Interactions*, Phys. Lett. **B69** (1977) 489.

[7] G. R. Farrar and P. Fayet, *Phenomenology of the Production, Decay, and Detection of New Hadronic States Associated with Supersymmetry*, Phys. Lett. **B76** (1978) 575.

[8] M. Dine, W. Fischler, and M. Srednicki, *Supersymmetric Technicolor*, Nucl. Phys. **B189** (1981) 575.

[9] S. Dimopoulos and S. Raby, *Supercolor*, Nucl. Phys. **B192** (1981) 353.

[10] L. Alvarez-Gaume, M. Claudson, and M. Wise, *Low-energy Supersymmetry*, Nucl. Phys. **B207** (1982) 96.

[11] C. R. Nappi and B. A. Ovrut, *Supersymmetric Extension of the SU(3)×SU(2)×U(1) Model*, Phys. Lett. **B113** (1982) 175.

[12] M. Dine, A. Nelson, Y.Nir, and Y. Shirman, *New Tools for Low-energy Dynamical Supersymmetry Breaking*, Phys. Rev. **D53** (1996) 2658, hep-ph/9507378.

[13] LEPSUSYWG, ALEPH, DELPHI, L3 and OPAL Experiments, *Combined LEP GMSB stau/smuon/selectron Results, 189-208 GeV*, Lepsusywg/02-09.2, 2002. http://lepsusy.web.cern.ch/lepsusy/.

[14] OPAL Collaboration, G. Abbiendi et al., *Searches for Gauge-Mediated Supersymmetry Breaking Topologies in $e^+ e^-$ Collisions at LEP2*, Eur.Phys.J. **C46** (2006) 307–341, arXiv:hep-ex/0507048 [hep-ex].

[15] CMS Collaboration, *Search for New Physics with Same-Sign Isolated Dilepton Events with Jets and Missing Transverse Energy at the LHC*, JHEP **1106** (2011) 077, arXiv:1104.3168 [hep-ex].

[16] CMS Collaboration, *Search for Physics Beyond the Standard Model Using Multilepton Signatures in pp Collisions at $\sqrt{s}$ = 7 TeV*, Phys.Lett. **B704** (2011) 411–433, arXiv:1106.0933 [hep-ex].

[17] CMS Collaboration, *Multileptonic SUSY Searches*, CMS-PAS-SUS-11-013, 2011. http://cdsweb.cern.ch/record/1393719.

[18] CMS Collaboration, *Search for Supersymmetry in All-Hadronic Events with Tau Leptons*, CMS-PAS-SUS-11-007, 2011. http://cdsweb.cern.ch/record/1401920.

[19] CMS Collaboration, *Search for New Physics with Same-Sign Isolated Dilepton Events with Jets and Missing Energy*, CMS-PAS-SUS-11-010, 2011. http://cdsweb.cern.ch/record/1370064.

[20] ATLAS Collaboration, *The ATLAS Experiment at the CERN Large Hadron Collider*, JINST **3** (2008) S08003.

[21] M. L. Mangano, M. Moretti, F. Piccinini, R. Pittau, and A. D. Polosa, *ALPGEN, a Generator for Hard Multiparton Processes in Hadronic Collisions*, JHEP **0307** (2003) 001, arXiv:hep-ph/0206293 [hep-ph].

[22] J. Pumplin, D. Stump, J. Huston, H. Lai, P. M. Nadolsky, et al., *New Generation of Parton Distributions with Uncertainties from Global QCD Analysis*, JHEP **0207** (2002) 012, arXiv:hep-ph/0201195 [hep-ph].

[23] S. Frixione and B. R. Webber, *Matching NLO QCD Computations and Parton Shower Simulations*, JHEP **0206** (2002) 029, arXiv:hep-ph/0204244 [hep-ph].

[24] S. Frixione, P. Nason, and B. R. Webber, *Matching NLO QCD and Parton Showers in Heavy Flavor Production*, JHEP **0308** (2003) 007, arXiv:hep-ph/0305252 [hep-ph].

[25] S. Frixione, E. Laenen, P. Motylinski, and B. R. Webber, *Single-top Production in MC@NLO*, JHEP **0603** (2006) 092, arXiv:hep-ph/0512250 [hep-ph].

[26] P. M. Nadolsky, H.-L. Lai, Q.-H. Cao, J. Huston, J. Pumplin, et al., *Implications of CTEQ Global Analysis for Collider Observables*, Phys. Rev. **D78** (2008) 013004, arXiv:0802.0007 [hep-ph].

[27] T. Sjostrand, S. Mrenna, and P. Skands, *PYTHIA 6.4 Physics and Manual*, JHEP **0605** (2006) 026, arXiv:hep-ph/0603175 [hep-ph].

[28] G. Corcella, I. Knowles, G. Marchesini, S. Moretti, K. Odagiri, et al., *HERWIG 6: An Event Generator for Hadron Emission Reactions with Interfering Gluons (Including Supersymmetric Processes)*, JHEP **0101** (2001) 010, arXiv:hep-ph/0011363 [hep-ph].

[29] J. Butterworth, J. R. Forshaw, and M. Seymour, *Multiparton Interactions in Photoproduction at HERA*, Z.Phys. **C72** (1996) 637, arXiv:hep-ph/9601371 [hep-ph].

[30] ATLAS Collaboration, *First Tuning of HERWIG/JIMMY to ATLAS Data*, ATL-PHYS-PUB-2010-014, Oct, 2010. http://cdsweb.cern.ch/record/1303025.

[31] S. Jadach, Z. Was, R. Decker, and J. H. Kuhn, *The Tau Decay Library TAUOLA, Version 2.4*, Comput. Phys. Commun. **76** (1993) 361.

[32] P. Golonka et al., *The Tauola-Photos-F Environment for the TAUOLA and PHOTOS Packages, Release II*, Comput. Phys. Commun. **174** (2006) 818.

[33] E. Barberio and Z. Was, *PHOTOS - a Universal Monte Carlo for QED Radiative Corrections: Version 2.0*, Comput. Phys. Commun. **79** (1994) 291.

[34] F. E. Paige, S. D. Protopopescu, H. Baer, and X. Tata, *ISAJET 7.69: A Monte Carlo Event Generator for pp, $\bar{p}p$, and e^+e^- Reactions*, arXiv:hep-ph/0312045.

[35] M. Bahr et al., *Herwig++ Physics and Manual*, Eur. Phys. J. **C58** (2008) 639–707, arXiv:0803.0883v3 [hep-ph].

[36] A. Sherstnev and R. S. Thorne, *Parton Distributions for LO Generators*, Eur. Phys. J. **C55** (2008) 553, arXiv:0711.2473 [hep-ph].

[37] *PROSPINO2*, http://www.thphys.uni-heidelberg.de/~plehn/index.php?show=prospino.

[38] W. Beenakker, R. Hopker, M. Spira, and P. Zerwas, *Squark and Gluino Production at Hadron Colliders*, Nucl. Phys. **B492** (1997) 51, arXiv:hep-ph/9610490 [hep-ph].

[39] W. Beenakker, M. Kramer, T. Plehn, M. Spira, and P. M. Zerwas, *Stop Production at Hadron Colliders*, Nucl. Phys. **B515** (1998) 3, arXiv:hep-ph/9710451 [hep-ph].

[40] W. Beenakker, M. Klasen, M. Kramer, T. Plehn, M. Spira, et al., *The Production of Charginos / Neutralinos and Sleptons at Hadron Colliders*, Phys. Rev. Lett. **83** (1999) 3780, arXiv:hep-ph/9906298 [hep-ph].

[41] M. Spira, *Higgs and SUSY Particle Production at Hadron Colliders*, arXiv:hep-ph/0211145 [hep-ph].

[42] T. Plehn, *Measuring the MSSM Lagrangean*, Czech. J. Phys. **55** (2005) B213–B220, arXiv:hep-ph/0410063 [hep-ph].

[43] GEANT4 Collaboration, S. Agostinelli et al., *GEANT4: A Simulation Toolkit*, Nucl. Instrum. Meth. **A506** (2003) 250.

[44] ATLAS Collaboration, *The ATLAS Simulation Infrastructure*, Eur. Phys. J. **C70** (2010) 823, arXiv:1005.4568 [physics.ins-det].

[45] M. Cacciari, G. P. Salam, and G. Soyez, *The anti-kt Jet Clustering Algorithm*, JHEP **04** (2008) 063, arXiv:0802.1189 [hep-ph].

[46] ATLAS Collaboration, *Jet Energy Measurement with the ATLAS Detector in Proton-Proton Collisions at* $\sqrt{s} = 7$ *TeV*, arXiv:1112.6426 [hep-ex]. Submitted to Eur. Phys. J. C.

[47] ATLAS Collaboration, *Electron Performance Measurements with the ATLAS Detector using the 2010 LHC Proton-Proton Collision Data*, arXiv:1110.3174 [hep-ex]. Submitted to Eur. Phys. J. C.

[48] ATLAS Collaboration, *Searches for Supersymmetry with the ATLAS Detector using Final States with Two Leptons and Missing Transverse Momentum in* $\sqrt{s} = 7$ *TeV Proton-Proton Collisions*, arXiv:1110.6189 [hep-ex]. Submitted to Phy. Lett. B.

[49] ATLAS Collaboration, *Performance of Missing Transverse Momentum Reconstruction in Proton-Proton Collisions at 7 TeV with ATLAS*, Eur. Phys. J. **C72** (2012) 1844, arXiv:1108.5602 [hep-ex].

[50] ATLAS Collaboration, *Performance of the Reconstruction and Identification of Hadronic Tau Decays with ATLAS*, ATLAS-CONF-2011-152, Nov, 2011. http://cdsweb.cern.ch/record/1398195.

[51] ATLAS Collaboration, *Luminosity Determination in pp Collisions at* $\sqrt{s} = 7$ *TeV using the ATLAS Detector in 2011*, ATLAS-CONF-2011-116, 2011. http://cdsweb.cern.ch/record/1376384.

[52] ATLAS Collaboration, *Luminosity Determination in pp Collisions at $\sqrt{s}$ = 7 TeV Using the ATLAS Detector at the LHC*, Eur. Phys. J. **C71** (2011) 1630, arXiv:1101.2185 [hep-ex].

[53] D. Stump, J. Huston, J. Pumplin, W.-K. Tung, H. Lai, et al., *Inclusive Jet Production, Parton Distributions, and the Search for New Physics*, JHEP **0310** (2003) 046, arXiv:hep-ph/0303013.

[54] A. L. Read, *Presentation of Search Results: The CL_s Technique*, J. Phys. **G28** (2002) 2693.